

# Quantum yields of hydroxyl radicals in illuminated TiO<sub>2</sub> nanocrystallite layers

Ruomei Gao<sup>a</sup>, Johannes Stark<sup>a</sup>, Detlef W. Bahnemann<sup>b</sup>, Joseph Rabani<sup>a,\*</sup>

<sup>a</sup> Department of Physical Chemistry and the Farkas Center, The Hebrew University of Jerusalem, Jerusalem 91904, Israel

<sup>b</sup> Department of Photocatalysis and Nanotechnology, Institute fuer Technische Chemie, Universitaet Hannover, Callinstrasse 3, D-30167 Hannover, Germany

Received 24 July 2001; received in revised form 5 December 2001; accepted 5 December 2001

## Abstract

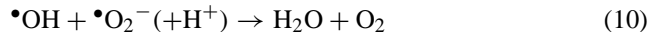
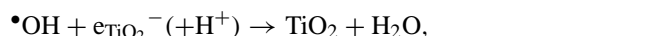
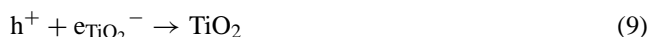
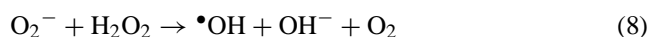
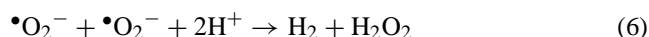
The yield of hydroxyl radicals has been determined by illumination of TiO<sub>2</sub> layers immersed in air saturated aqueous methanol solutions. This yield is equal to half the measured formaldehyde yield in the pH range 7–13. A detailed mechanism is proposed, accounting for the lack of accumulation of hydrogen peroxide. The effect of changing methanol concentration, pH and light intensity (the latter by three orders of magnitude) is in agreement with a very simple mechanism. In contrast to hydroxyl radicals, which react via hydrogen abstraction, leading to formation of HCHO, there is no sign for reaction of methanol with mobile holes. Thus, the limiting quantum yield observed at high methanol concentration is related to the maximum yield of •OH<sub>ads</sub> under air saturated conditions at the given pH and light intensity. The effect of light intensity shows the expected inverted square root dependency. The yield of •OH<sub>ads</sub> is nearly constant in the range 7 < pH < 12. This system may be useful for comparative tests of different TiO<sub>2</sub> preparations. © 2002 Elsevier Science B.V. All rights reserved.

**Keywords:** Titanium dioxide; Photocatalysis; Thin layers; Hydroxyl radical; Quantum yield

## 1. Introduction

A growing interest in photoelectrochemistry and photocatalytic oxidation of organic compounds follows the pioneering works of Gerischer [1], Fujishima and Honda [2]. Photocatalytic detoxification of organic pollutants with the aid of TiO<sub>2</sub> particles or layers is a promising tool for purification and sterilization of environmental aqueous media [3–9]. Absorption of a photon with energy greater than the band gap energy results in the formation of conduction band electron and valence band hole, according to reaction (1). It is commonly accepted that the hole is quickly converted to the hydroxyl radical upon oxidation of surface water, according to reaction (2), and that the hydroxyl radical is the major reactant, which is responsible for oxidation of organic substrates. Convincing evidence for the generation of •OH<sub>ads</sub> (as well as bulk •OH) has been obtained from photochemical (TiO<sub>2</sub>) and radiation chemical studies involving addition of •OH radicals to phenol, in comparison to electron transfer oxidation of phenol by TiO<sub>2</sub> holes and by strong oxidants [10]. Spin trapping techniques, using •OH scavengers to produce a free radical [11–15] or using a stable free radical to scavenge •OH [16], have been used to investigate

reaction mechanisms and quantum yields. These methods, however, require independent knowledge of the chemical yield of •OH reaction at the desired site, as well as the detailed reaction mechanism in order to distinguish between reactions of •OH radicals and holes.



(Although the initial reactions of •OH and holes are different, the end products may be the same). Sun and Bolton [17]

\* Corresponding author.

E-mail address: rabani@vms.huji.ac.il (J. Rabani).

used methanol as an  $\bullet\text{OH}$  scavenger and studied the rate of build up of formaldehyde as a measure of the hydroxyl radical yield. In the presence of methanol, the  $\bullet\text{OH}$  radical reacts predominantly by H atom abstraction according to reaction (3). When oxygen is also present,  $e_{\text{TiO}_2}^-$  and the organic radical  $\bullet\text{CH}_2\text{OH}$  react with it producing (at  $\text{pH} > 5$ )  $\bullet\text{O}_2^-$  radical ions and the peroxy radical  $\bullet\text{O}_2\text{CH}_2\text{OH}$ , respectively (reactions (4) and (5)). The peroxy radical decomposes to the stable HCHO, releasing additional  $\bullet\text{O}_2^-$  radical ions. Subsequently, dismutation of  $\bullet\text{O}_2^-$  takes place (reaction (6)) via disproportionation of  $\bullet\text{O}_2^-$  with  $\text{HO}_2\bullet$ . The product of reaction (6) is hydrogen peroxide, which may further react according to reaction (7), although the Haber–Weiss chain decomposition (8) cannot be ruled out. Thus, the yield of formaldehyde,  $\Phi_{\text{HCHO}} = 2\Phi_{\text{OH}}$ .  $\Phi_{\text{OH}} = 0.04$  has been reported in  $\text{TiO}_2$  (Aldrich) powder at neutral pH by Sun and Bolton [17]. Since the fate of hydrogen peroxide under the conditions of the measurements is not clear, the actual yield may be as low as 0.02. The smaller than 1 values of  $\Phi$  reflect electron–hole recombination, competing with reactions with the scavengers (methanol and oxygen, respectively).

In the present manuscript we report studies of  $\Phi_{\text{OH}}$  in  $\text{TiO}_2$  layers, as a function of scavenger concentration and absorbed light intensity, in the pH range 7–13, using methanol as  $\bullet\text{OH}$  scavenger.

## 2. Experimental

### 2.1. Materials

NaOH (Frutarom),  $\text{HClO}_4$  (Baker),  $\text{Na}_2\text{HPO}_4$  (Sigma),  $\text{NaH}_2\text{PO}_4$  (BDH),  $\text{Na}_2\text{CO}_3$  (Baker),  $\text{NaHCO}_3$  (Frutarom) were used as received. Phosphate buffer (0.03 M) was used to adjust the pH between 7 and 9. Carbonate/Bicarbonate (0.012 M) was used between pH 9 and 11, while pHs  $> 11$  were adjusted using NaOH. An Orion Ross combination glass electrode was used for pH measurements ( $\pm 0.01$  pH units at  $25^\circ\text{C}$ ).

### 2.2. Layers

$\text{TiO}_2$  colloidal solution was prepared by hydrolysis of titanium 2-propoxide (Aldrich) slightly modifying the reported procedure [18]. The resulting suspension was heated at pH 2.5 ( $\text{HNO}_3$ ) for several days at  $80^\circ\text{C}$  until a clear solution was observed, yielding nanocrystallites with average diameter of 5 nm. Solutions containing 200 g/l ( $D_{355}$  of a 1/1000 solution was 0.13) were used for the preparations of thin layers on ITO by successive spin coatings (1 min at 3500 rpm). Three coatings were used for the preparation of  $\text{TiO}_2$  layer with optical absorption 0.3 at 355 nm. Layer dimensions were  $(0.9 \pm 0.05) \times (2.5 \pm 0.1) \text{ cm}^2$ , with thickness of  $1 \pm 0.15 \mu\text{m}$ .

### 2.3. Illumination

The excitation light source was a 75 W Xe lamp. The light was filtered by Pyrex glass (2 mm thick, cutting below 300 nm) and Oriel 59800 cut-off filter (transmitting below 400 nm). The light intensity was adjusted by appropriate neutral density filters, and was monitored by an OPHIR NOVA 10A-P-SH during illumination to assure stability of the light. A water filter (9.5 cm) was used to minimize heating by the IR irradiation. The illumination area was  $1.2 \text{ cm}^2$ .

### 2.4. The reaction cell

Experiments were carried out in a closed  $5 \text{ cm}^3$  cell with Pyrex windows containing  $4 \text{ cm}^3$  air saturated solution in water. Usually 0.2 M methanol was used as  $\bullet\text{OH}$  scavenger. The  $\text{TiO}_2$  layer was near to the optical window from which the light entered, with the  $\text{TiO}_2$  coated side facing the solution. The layer was pre-equilibrated with the solution in the dark by mixing (magnetic stirrer) during 20 min prior to illumination. Mixing continued during illumination.

### 2.5. Formaldehyde

Formaldehyde was determined by the Nash method [19], based on the Hantzsch reaction: 15  $\mu\text{l}$  acetylacetone was added to 3 ml solution, consisting of 1.5 ml sample and 1.5 ml of 0.18 M ammonium phosphate buffer at pH 6.0. Spectrophotometric measurements were carried out at 412 nm ( $\epsilon = 8000 \text{ M}^{-1} \text{ cm}^{-1}$ ) using Kontron's Uvikon 860 spectrophotometer.

The amount of absorbed light was determined from the decrease in light intensity observed upon replacing a bare ITO glass with one coated  $\text{TiO}_2$ , using the  $\text{Fe}^{3+}$  oxalate actinometer [20,21].

## 3. Results and discussion

Formation of HCHO was nearly linear with the time of illumination under the conditions used (absorbed light intensity varied from  $2.3 \times 10^{-11}$  to  $2.1 \times 10^{-8} \text{ ein s}^{-1} \text{ cm}^{-2}$ ). Effect of methanol concentration on the quantum yield of formaldehyde shows that a near plateau value is reached at 2 M methanol, as shown in Fig. 1. Although  $\Phi_{\text{HCHO}}$  depend on light intensity and pH, a plateau at  $[\text{CH}_3\text{OH}] > 2 \text{ M}$  is observed in the entire pH and intensity range. Therefore this concentration was used for comparative studies of the effects of pH and light intensity.

The yield of formaldehyde is determined by a set of two pairs of competing reactions. First, competition between hole trapping (reaction (2)) and hole recombination with the electron according to reaction (9). It is suggested that methanol does not react with the hole so that this competition depends on the local concentrations of the electrons

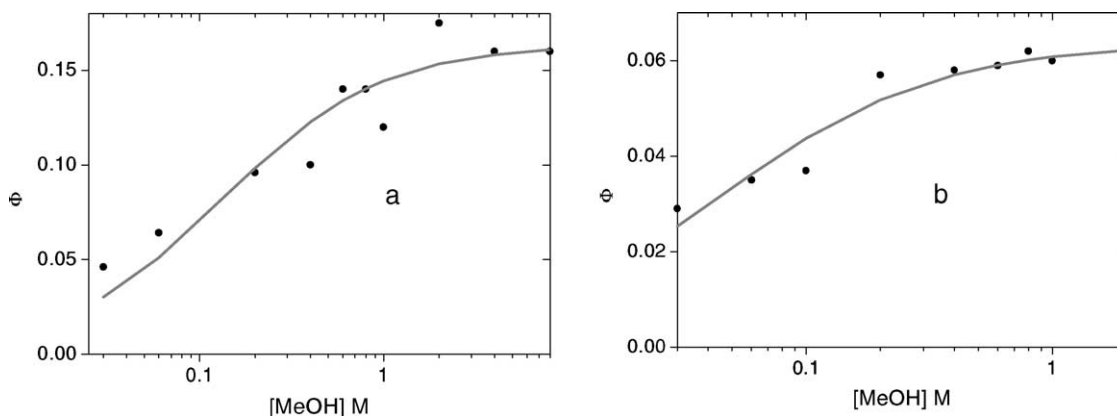


Fig. 1. HCHO yield as a function of methanol concentration; pH = 10.3 ( $4 \times 10^{-2}$  M carbonate). Solid line represents (a) light intensity  $7.8 \times 10^{-10}$  ein/s, best fit obtained with  $\Phi_{\max} = 0.162$ ,  $k_c = 0.155 \text{ M}^{-1}$ . (b) Light intensity  $8.1 \times 10^{-9}$  ein/s, best fit obtained with  $\Phi_{\max} = 0.064$ ,  $k_c = 0.045 \text{ M}^{-1}$ .

and holes in the  $\text{TiO}_2$  layer but not on methanol concentration. The second pair of competing reactions involves reaction (3) and (10). This competition is determined by the local  $\bullet\text{OH}$  and  $e_{\text{TiO}_2}^-$  as well as by the methanol concentrations. The equation used for the calculation of the solid line in Fig. 1,  $\Phi_{\text{HCHO}} = \Phi_{\max}/(1 + k_c/[\text{CH}_3\text{OH}])$ , is based on a simple competition between reactions (3) and (10), ignoring possible reactions of  $e_{\text{TiO}_2}^-$  and other intermediates.  $\Phi_{\max}$  is the quantum yield at the plateau of Fig. 1. The constant  $k_c$  includes the reciprocal of the square root of the light intensity,  $I^{-1/2}$ , which is constant under the conditions of Fig. 1. Dependency of product yield on  $I^{-1/2}$  is well known in many systems [22–25], although in some cases the rate has been reported to depend linearly on intensity [26]. A general kinetic scheme describing the essential features of steady state photocatalysis predicting the decrease of quantum yield upon increasing illumination intensity has been proposed by Gerischer [27,28]. In the absence of detailed information on the kinetic parameters, which affect the yield in the present system, the above simple equation was used, showing very good fit with the results.

The lack of methanol reaction with  $\text{h}^+$  is in agreement with a plateau  $<1$  observed in Fig. 1. It may be argued that holes react with methanol, yielding products other than HCHO. Abstraction of an electron is expected to produce at first the radical ion  $(\text{CH}_3\text{OH}^+)^\bullet$  [29], which may subsequently produce  $\text{CH}_3\text{O}^\bullet$  or  $\bullet\text{CH}_2\text{OH}$  (deprotonation). Both  $(\text{CH}_3\text{OH}^+)^\bullet$  and  $\text{CH}_3\text{O}^\bullet$  are able to quickly recombine with  $e_{\text{TiO}_2}^-$ . If these intermediates eventually produce HCHO, the limiting quantum yield (ignoring the formation of additional  $\bullet\text{OH}$  by reactions (7) and (8)) must be 1. If only a fraction of  $(\text{CH}_3\text{OH}^+)^\bullet$  and  $\text{CH}_3\text{O}^\bullet$  produce HCHO, and the rest recombines with  $e_{\text{TiO}_2}^-$ , the limiting  $\Phi_{\text{HCHO}} < 1$  is expected. In the latter case, however, the limiting yield should not depend on the light intensity, contrary to the experimental results of Fig. 1, showing  $\Phi_{\text{HCHO}}(\text{limiting}) = 0.162$  at  $7.8 \times 10^{-10}$  ein/s and  $\Phi_{\text{HCHO}}(\text{limiting}) = 0.064$  at  $8.1 \times 10^{-9}$  ein/s. Note that  $\Phi_{\max}$  (Fig. 1) changes with the square root of the light intensity, as might be expected

by competition between reactions (2) and (9), which determine the yield of  $\bullet\text{OH}$ . The parameter  $k_c$  is determined by the competition between reactions (3) and the  $\bullet\text{OH}$  reduction reactions (10). The three fold variation of  $k_c$  when the intensity changes by a factor of ten, is expected on the basis of the proposed mechanism.

The effect of light intensity on  $\Phi_{\text{HCHO}}$  is shown more directly in Fig. 2 at constant methanol concentration. Again, simple competition between reactions (2) and (9) is assumed. This is justified since Fig. 2 represents conditions where practically all  $\bullet\text{OH}$  radicals are scavenged by the 2 M methanol, and the only competition is between reactions (2) and (9). The good agreement between the experimental data and the fitted line is useful for comparison between different conditions such as light intensity effects at different pHs.

Analysis for hydrogen peroxide in the illuminated systems detected only negligible concentrations. Therefore, the  $\bullet\text{OH}$  radicals produced by reaction (7) double the yield of HCHO so that  $\Phi_{\max} = 2$ . We have carried out quantum yield mea-

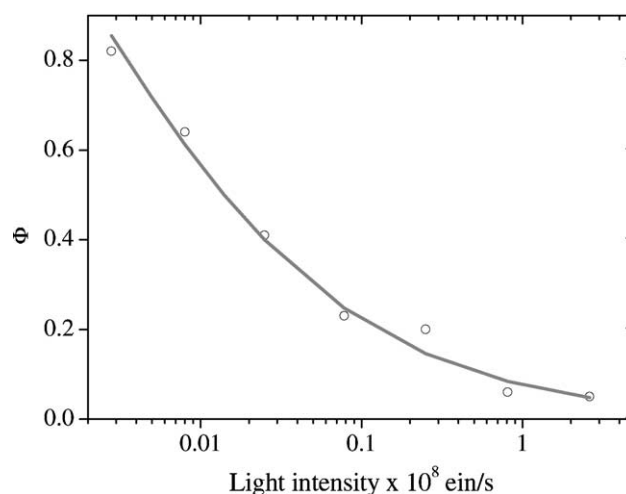


Fig. 2.  $\Phi_{\text{HCHO}}$  as a function of light intensity. 2 M  $\text{CH}_3\text{OH}$ , pH 11. The solid line represents the equation  $\Phi_{\text{HCHO}} = 2/(1 + k_1 I^{1/2})$ , with  $k_1 = (2.53 \pm 0.1) \times 10^5 \text{ s/ein}$ .

Table 1  
Competition between reactions (2) and (9) at different pHs<sup>a</sup>

	pH					
	7	8	10.3	11	12.2	13
$k_1$ ( $\times 10^5$ s <sup>1/2</sup> ein <sup>-1/2</sup> )	2.5	~5	4	2.5	4	7
$\Phi_{\text{HCHO}}^b$	0.64	0.57	0.43	0.5	0.5	0.37

<sup>a</sup> The 2 M CH<sub>3</sub>OH values of  $k_1$  are best fits obtained from results similar to those presented in Fig. 2. The yields used for the calculation of average  $\Phi_{\text{HCHO}}$  are reproducible within  $\pm 20\%$ .

<sup>b</sup> Light intensity  $2.8 \times 10^{-11}$  ein/s per cm<sup>2</sup>.

measurements as a function of light intensity in a wide range of pHs from 7 to 13. The effect of intensity is similar in the entire range, with apparent deviations at high intensities at pH 13. The resulting values of  $k_1$  are summarized in Table 1.

At any given pH, the same electrode was used for the entire set of intensities. Since the electrodes may be somewhat different in dimensions, results obtained with the same electrode are more reliable for comparative tests. Average yields obtained with different electrodes are shown in the third row of Table 1. The pH effect indicates constant  $\bullet\text{OH}$  yield or moderate decrease with increasing pH in the range 7–12.2, and lower yield at pH 13. Similarly, the results of  $k_1$  show stable or moderate increase with pH in the range 7–12.2, and a sharp increase at pH 13. Note that while the reported  $\Phi_{\text{HCHO}}$  in Table 1 represents results at  $2.8 \times 10^{-11}$  ein/s per cm<sup>2</sup>,  $k_1$  is derived from the entire range of intensities at any given pH.

The redox potentials of  $\bullet\text{OH}$  and  $\text{h}^+$  decrease by 0.059 V upon increasing the pH by 1 unit, so that the driving force for reaction (2) is expected to be pH independent. Note that the quantum yield of HCHO, from which the yield of  $\bullet\text{OH}$  radicals is derived, may be affected by secondary reactions. These include possible radical ionic dissociation at the high alkali pH as well as specific effects of the buffers used. Attempts to study the effect of buffers were inconclusive, because of the large scatter of results.

#### 4. Conclusions

The yield of  $\bullet\text{OH}$  radicals depends on the competition between oxidation of surface water by the holes and electron–hole recombination. This yield can be estimated from measurements of formaldehyde [17] using >2 M CH<sub>3</sub>OH, which under our conditions is a sufficient concentration for total scavenging of the  $\bullet\text{OH}$  radicals. In the presence of oxygen, the methanol radicals are converted to formaldehyde, along with  $\bullet\text{O}_2^-$  radical ions. The latter produce hydrogen peroxide by dismutation. Additional hydrogen peroxide is produced via direct reaction of oxygen with the TiO<sub>2</sub> electrons. Since analysis of H<sub>2</sub>O<sub>2</sub> in the illuminated systems showed only small concentrations of H<sub>2</sub>O<sub>2</sub> (<10 and 2% of the measured formaldehyde concentrations at pH 7 and 12.2, respectively), it is evident that the

hydrogen peroxide is destroyed, apparently by reaction (11) or by the Haber–Weiss reaction (12). In either case  $\bullet\text{OH}$  radicals are produced, which eventually double  $\Phi_{\text{HCHO}}$ . Therefore, the hydroxyl radical yield must be only half of the formaldehyde yield reported in this (and previous) [17] work.



Reduction of  $\bullet\text{O}_2^-$  by the TiO<sub>2</sub> electrons is also possible, although it is expected to affect the  $\Phi_{\text{HCHO}}/\Phi_{\bullet\text{OH}}$  ratio in the same way as reactions (11) and (12).

At the highest light intensity,  $\sim 0.2$  M electron–hole pairs are generated in 1 s. Taking the average diameter of the nanocrystallites 5 nm, an average of  $\sim 10$  electron pairs is produced in a nanocrystallite each second. The steady state concentration of  $\text{h}^+$  is several orders of magnitude lower. This means that under the steady state conditions of the illumination, each TiO<sub>2</sub> nanocrystallite has no more than one electron–hole pair, ruling out the possibility of a second-order rate law for recombination. Consequently, the micro-volume relevant for the competition between reactions (2) and (9) is orders of magnitude larger than that of a single nanocrystallite.

Although the present study does not discriminate between trapped and conduction band electrons, it is possible to conclude that due to the relatively low concentrations of O<sub>2</sub> and H<sub>2</sub>O<sub>2</sub>, their reactions with the TiO<sub>2</sub> electron must be much slower than the reaction of  $\bullet\text{OH}$  with methanol [30,31]. Reaction rates of these scavengers have been determined [32,33], although it is not clear whether these reactions represent conduction band electrons. The competition between reactions (3) and (10) can be expected to depend on the relative contributions of the reducing intermediates and the concentration of the electron scavengers, so that the actual value of  $\Phi_{\bullet\text{OH}}$  may be different in other, similar systems, depending on conditions and the nature of  $\bullet\text{OH}$  scavengers.

Further work is in progress on different TiO<sub>2</sub> preparations and different hydroxyl radical and TiO<sub>2</sub> electron scavengers, in order to define a general reliable standard for photocatalytic efficiency.

#### Acknowledgements

This work was funded by the European Commission under the Energy, Environment and Sustainable Development programme, contract number EVK1-CT-2000-00077. We are indebted to E. Gilead and Y. Ozeri for their technical assistance.

#### References

- [1] H. Gerischer, Photochem. Photobiol. 16 (1972) 243.
- [2] A. Fujishima, K. Honda, Bull. Chem. Soc. Jpn. 44 (1971) 1148.

- [3] M.R. Hoffmann, S.T. Martin, W. Choi, D.W. Bahnemann, *Chem. Rev.* 95 (1995) 69.
- [4] N. Serpone, R.F. Khairutdinov, *Semicond. Nanoclusters Phys. Chem. Catal. Aspects* 103 (1997) 417.
- [5] E. Pelizzetti, C. Minero, *Coll. Surf. Physicochem. Eng. Aspects* 151 (22) (1999) 321.
- [6] A. Mills, R.H. Davies, D. Worsley, *Chem. Soc. Rev.* (1993) 417.
- [7] D.F. Ollis, C. Turchi, *Environ. Prog.* 9 (1990) 229.
- [8] M.A. Fox, M.T. Dulay, *Chem. Rev.* 93 (1993) 341.
- [9] A. Fujishima, K. Hashimoto, T. Watanabe, *TiO<sub>2</sub> Photocatalysis Fundamentals and Applications*, BKC, Inc., Tokyo, 1999.
- [10] S. Goldstein, G. Czapski, J. Rabani, *J. Phys. Chem.* 98 (1994) 6586.
- [11] C.D. Jaeger, A.J. Bard, *J. Phys. Chem.* 83 (1979) 3146.
- [12] J.R. Harbour, V.S.F. Chow, J.R. Bolton, *Can. J. Chem.* 52 (1974) 3549.
- [13] G.V. Buxton, C.L. Greenstock, W.P. Helman, A.B. Ross, *J. Phys. Chem. Ref. Data* 17 (1988) 717.
- [14] M.A. Grela, M.E.J. Coronel, A.J. Colussi, *J. Phys. Chem.* 100 (1996) 16940.
- [15] G. Riegel, J.R. Bolton, *J. Phys. Chem.* 99 (1995) 4215.
- [16] P.F. Schwarz, N.J. Turro, S.H. Bossmann, A.M. Braun, A.A. Abdel Wahab, H. Duerr, *J. Phys. Chem.* 101 (1997) 7127.
- [17] L.Z. Sun, J.R. Bolton, *J. Phys. Chem.* 100 (1996) 4127.
- [18] M.K. Nazeeruddin, A. Kay, I. Rodicio, R. Humphry-Baker, E. Muller, P. Liska, N. Vlachopoulos, M. Graetzel, *J. Am. Chem. Soc.* 115 (1993) 6382.
- [19] T. Nash, *Biochemistry* 55 (1953) 416.
- [20] C.G. Hatchard, C.A. Parker, *Proc. Roy. Soc. Ser. A* 235 (1956) 518.
- [21] J.N. Demas, W.D. Bowman, E.F. Zalewski, R.A. Valapoldi, *J. Phys. Chem.* 85 (1981) 2766.
- [22] A.J. Hoffman, E.R. Carraway, M.R. Hoffmann, *Environ. Sci. Technol.* 28 (1994) 776.
- [23] Y. Inel, A.N. Okte, *J. Photochem. Photobiol. A* 96 (1996) 175.
- [24] Y. Nosaka, M.A. Fox, *J. Phys. Chem.* 90 (1986) 6521.
- [25] N. Serpone, G. Sauve, R. Koch, H. Tahiri, P. Pichat, P. Piccinini, E. Pelizzetti, H. Hidaka, *J. Photochem. Photobiol. A* 94 (1996) 191.
- [26] A. Mills, A. Belghazi, R.H. Davies, D. Worsley, S. Morris, *J. Photochem. Photobiol. A* 79 (1994) 131.
- [27] H. Gerischer, *Electrochim. Acta* 38 (1993) 3.
- [28] H. Gerischer, *Electrochim. Acta* 40 (1995) 1277.
- [29] J. Rabani, K. Yamashita, K. Ushida, J. Stark, A. Kira, *J. Phys. Chem. B* 102 (1998) 1689.
- [30] W.G. Mallard, A.B. Ross, W.P. Helman, *NIST Standard References Database 40, Version 3.0*, 1998.
- [31] P. Neta, R. Huie, A.B. Ross, *J. Phys. Chem. Ref. Data* 17 (1988) 1027.
- [32] D.W. Bahnemann, M. Hilgendorff, R. Memming, *J. Phys. Chem. B* 101 (1997) 4265.
- [33] R. Gao, A. Safrany, J. Rabani, *Radiation Physics and Chemistry*, to be published.